A MODEL FOR GPS-GDOP PREDICTION IN URBAN ENVIRONMENT USING LIDAR DATA

Bharat Lohani and Raman Kumar
Department of Civil Engineering, IIT Kanpur, Kanpur 208016 (India)
blohani@iitk.ac.in

KEY WORDS: LiDAR, GDOP, GPS Signal, GPS accuracy, LBS, predictive modeling.

ABSTRACT
This paper attempts to develop a model which can, using LiDAR data, predict GDOP at a point in space and time. LiDAR data are used to classify the terrain around a receiver in categories like ground, opaque objects, translucent objects and transparent as per their response to transmission of GPS signals. Through field experiment it has been established that Ultra Rapid Product (URP) can be satisfactorily used to determine GDOP in advance. Further experiments have shown that the translucent objects (mainly trees here) lower the GDOP quality. With the help of field experiments, the LiDAR data density on trees has been employed to provide each tree with a value that describes the probability that a satellite which is behind the tree is visible at the receiver. A model is presented which, for all possible combinations of visible satellites, computes the GDOP value along with the probability of occurrence of this GDOP.

1 INTRODUCTION

The present advancements are aiming at putting GPS as an integral component of several systems, which will rely on the GPS-determined-location for their functioning. The performance of these systems will depend on the positional accuracy achievable using the GPS. GPS accuracy is affected by the presence of obstructions in the form of buildings, trees and natural topography, as the GPS signals, being microwaves in radio frequency, suffer from signal masking or complete signal blockage due to these obstructions (MacGougan et al., 2001). The availability of GPS satellites and their configuration also plays an important role besides other factors. MacGougan et al. (2001) have shown the effect of signal masking through field experiment and observed that masking reduces the visibility to satellites. Further, the probability of seeing more satellites simultaneously reduces due to masking. The effect of trees on position has been studied by Hasegawa and Yoshimura(2003). The major effect of obstructions is lowering of signal by noise ratio (SNR), multipath and complete blockade of satellites.
For successful operation of GPS embedded devises it is desirable that the achievable accuracy can be predicted in advance. A few attempts have been made in this direction (Germroth and Carstensen, 2005; Sub, 2004). However, in these attempts GIS data with only buildings as obstructions have been used. The effect of trees has been not considered specifically.
With the availability of LiDAR data new possibilities have emerged for modelling the 3D structure of landscape at a large scale. LiDAR data are capable of identification of buildings and trees and offer a potential for their use in modelling the satellite visibility. In view of this an attempt has been made in this paper to use LiDAR data for predicating GPS satellite visibility and its role in GPS positional accuracy through the parameter of GDOP. Though, the obstructions in the form of buildings, trees and others introduce multipath, lower SNR, and cause diffraction these have not been considered in the present paper. The present paper investigates only the satellite visibility and consequent GDOP availability.

2 OBJECTIVES:

The main aim of this paper is to present a model to predict at a time in future the probability of getting a GDOP at any location in space. To realise this the following sub-objectives have been outlined:

1. Understanding the accuracy of GDOP computation using Ultra Rapid Product (URP)
2. Investigating the effect of trees on GDOP
3. Investigating the effect of different canopy densities on GDOP
4. LiDAR data processing to classify terrain in categories opaque, translucent and transparent for GPS signal.
5. Development of a model for satellite visibility based on URP.
6. Integration of above to generate a probability value for GDOP at a point in space and time in future.

3 LIDAR DATA AND INSTRUMENTS USED

It was planned to use the LiDAR data of IIT Kanpur campus which is essential for the full design of this paper. However, due to delay in planned data collection the LiDAR data provided by Optech Inc. of Niagra Fall have been used. The data were collected in 2004 using ALTM sensor. The airplane flew at an average height of 1190m, with a DSS 301 SN0039 camera on board for the aerial photographs. The average density of the LiDAR data is 2.74 points per square metre. For computational convenience, the data were subset.

To relate with the field experiment it was required to have LiDAR data of the trees employed in this paper. These data were simulated by carrying out measurements over trees using a Trimble reflector-less total station which was configured to generate coordinates in ECEF WGS-84 system.

Leica SR-530 dual frequency carrier phase GPS was used for field GDOP measurements. SkiPro software from Leica was used for processing of GPS data and to yield GDOP.

The aim of this paper is to predict GDOP for future. This requires the satellite ephemerides in advance. A number of products are available. However, the Ultra Rapid Product (URP) was chosen, as the requirement of this paper was an accurate product which can be used for prediction in immediate future. This data is downloadable in SP3 format, where data are available at a sampling of 15 minutes. The orbits were interpolated to generate data at a finer sampling.

4 THEORETICAL BACKGROUND

As shown in figure 1, a GPS ideally can see satellites anywhere in space (S) above horizon. However, due to presence of obstructions in the form of ground topography (G), above-ground objects (O) (like buildings), which are opaque for GPS signal the satellites behind these with respect to the location of receiver will not be visible. All other above ground objects (L) (like trees) will cause partial masking of GPS signal. Thus the signal availability is a function of the translucency of these objects. The satellites available in rest of the space (T) will be visible to the receiver.

We can define a set S as:

$$S = \{T, L, O, G\}$$

Further, each of these space components may be made of sub-space components as:

$$S = \{\{T_1, T_2, \ldots, T_n\}, \{L_1, L_2, \ldots, L_n\}, \{O_1, O_2, \ldots, O_n\}, \{G_1, G_2, \ldots, G_n\}\}$$

At any point in space and time (s, t), the set of satellite vehicles (SVs) behind a space component (say L_i) with respect to the receiver is:

$$l_i = \{ l_{1i}, l_{2i}, \ldots, l_{mi} \}$$

The GDOP at a point in space and time (s,t) (i.e. $GDOP_{(s,t)}$) will depend on the geometry of the satellites visible at the receiver. The SVs hidden by O and G will not participate in GDOP calculation, while the SVs in space T will be fully available. For the SVs behind translucent objects (L_i) it will depend upon whether the satellites l_{ji} are visible or not. The visibility of l_{ji} is a factor of the translucency of L_i . Depending the translucency of these objects a probability can be assigned to each of L_i as P_{Li} .

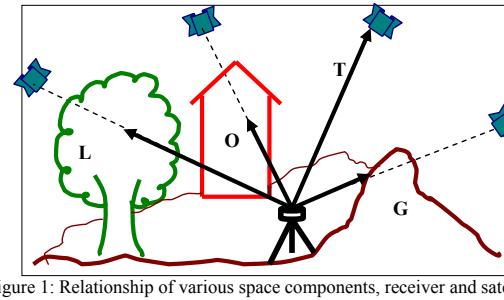

Figure 1: Relationship of various space components, receiver and satellites.

In view of the above the GDOP at a point (s,t) is $GDOP_{(s,t)} = f(\{t_i, l_i\}, P_{Li})$, where i =1 to n i.e. for all relevant T and L space components (s,t). Where $t_i = \{ t_{1i}, t_{2i}, ..., t_{mi} \}$ is the set of SVs behind space component T_i and $l_i = \{ l_{1i}, l_{2i}, ..., l_{mi} \}$ is the set of SVs behind space component L_i .
While SVs in t_i , for i = 1 to n, are always visible, the SVs in l_i , for i= 1 to n, may be or may not be visible depending the probability P_{Li} . Various scenarios of visibility that are possible within the set $\{ t_i , l_i \}$ are:

$$t_i \cup {}^{li}C_k \quad \text{where } k \in l_i \text{ and } 1 \le |k| \le |l_i| .$$

If E_i is an event set then : $E_i \in \left\{ t_i \cup {}^{li}C_k \right\}$

Let one such event is E=$\{ t_{11}, t_{2,1}, t_{12}, l_{11}, l_{12}, l_{22}, l_{32} \}$. This means, there are two transparent space elements T_1 and T_2 , while behind the first the SVs are t_{11} and $t_{2,1}$ behind the second there is only one SV i.e. t_{12} . Further, There are 2 translucent components i.e., L_1 and L_2., with SVs l_{11} and l_{12}, l_{22}, l_{32} being behind them, respectively. In addition, let the SVs l_{21} and l_{42} are not visible, though these are available behind L_1 and L_2, respectively. The probability of success of such event is:

$$P(E) = 1 \times 1 \times 1 \times P_{L1} \times P_{L2} \times P_{L2} \times P_{L2} \times (1 - P_{L1}) \times (1 - P_{L2})$$

The resulting GDOP for event E thus will have a probability P(E) | $\sum P(E_i)$=1.
Using the aforesaid a table can be generated for all possible events (E_i) their respective GDOP ($GDOP_{Ei}$) and probability of success of these events $P(E_i)$. For events yielding the same GDOP the probability will be added as each event is independent and mutually exclusive. The azimuth and elevation to a SV or a point in space with respect to receiver position and the GDOP can be computed by the standard approach not being presented here.

5 METHODOLOGY

5.1 GDOP computation using Ultra Rapid Product

The objective is to prove that URP data can be used for computing GDOP for a point in time in future. An experiment was set up where a GPS receiver was kept at a known location. This location was so chosen that there is no obstruction above 15° of horizon. GPS data were collected on four dates for around two hours each day. The data were collected at a sampling of 15 minutes which is same as the sampling rate of URP in SP3 file. The GDOP values were calculated for the above location using satellites that are above 15° of horizon in URP data.

The GDOP values computed from URP data and observed in the field are compared. The results are shown in table 1. The mean difference is 0.07 with a standard deviation of 0.25. This proves that URP can be used to predict the GDOP with sufficient accuracy.

Table 1: Comparison of Observed and Computed GDOP

Date	Time (Local)	Time (UTC)	GDOP (Observed by receiver)	GDOP(from URP)	Diff in GDOP
31/8/2006	10.30	05.00	2.00	2.02	-0.02
	11.15	05.45	2.10	2.09	0.01
	11.30	06.00	2.30	2.36	-0.06
	11.45	06.15	1.80	1.80	0.00
	12.00	06.30	2.00	1.92	0.08
	12.15	06.45	2.00	2.00	0.00
01/9/2006	10.00	04.30	2.30	2.35	-0.05
	10.15	04.45	2.30	2.02	0.28
	10.30	05.00	2.00	2.00	0.00
	11.00	05.30	3.80	3.80	0.00
	11.15	05.45	2.90	1.65	1.25
	11.30	06.00	2.90	2.45	0.45
04/9/2006	18.30	13.00	1.50	1.50	0.00
	19.00	13.30	1.90	1.92	-0.02
	19.15	13.45	1.90	1.92	-0.02
	19.30	14.00	2.50	2.45	0.05
	19.45	14.15	3.60	3.61	-0.01
	20.00	14.30	2.50	2.54	-0.04
	20.15	14.45	2.50	2.50	0.00
	20.30	15.00	2.20	2.20	0.00
07/9/2006	17.15	11.45	2.30	2.28	0.02
	18.00	12.30	1.90	1.97	-0.07
	18.15	12.45	2.20	2.17	0.03
	19.00	13.30	1.90	1.90	0.00
	19.15	13.45	1.90	1.90	0.00

5.2 Effect of trees on GDOP

Majority of above ground objects which are translucent for GPS signal are the trees. The aim of this experiment was to observe the affect on GDOP when the SVs are masked by the trees. Two trees with different canopy types (dry:tree1, dense leaves:tree2) were selected for this experiment. GPS receiver was placed at a known location besides the tree and GPS data were collected at a sampling of 1 minute for 12 hours. The receiver location was chosen such that GPS signals are masked only by the selected trees. The URP data were sub-sampled at 1 minute rate using interpolation. The theoretical GDOPs were computed for entire duration of 12 hours at a sampling of 1 minute. These are compared with the observed GDOP. The difference of observed and calculated GDOPs are determined and plotted in figure 2.

The positive values of differences in GDOP in the plot show that the GDOP values observed in field are consistently larger than the computed from URP data. The following table shows statistics of these differences and exhibits the effect of trees on GDOP. Further, the effect of tree with dense leaves (thick canopy) is significantly large.

Table2: Statistics of GDOP differences

	Tree1: Dry tree	Tree3: Dense leaves
Mean	0.23	0.54
Standard deviation	0.35	0.11
Maximum	31. 68	35.18

1.1. Effect of different canopy densities on GDOP

Two kinds of trees are selected for this purpose-first with thick canopy and second with thin leaves or no leaves. Observations were taken by placing the receiver near the trees. The observations were

taken at a sampling rate of 1 minute for 12 hours. All the SVs that are visible to receiver are recorded. This includes the SVs in space components T and L.

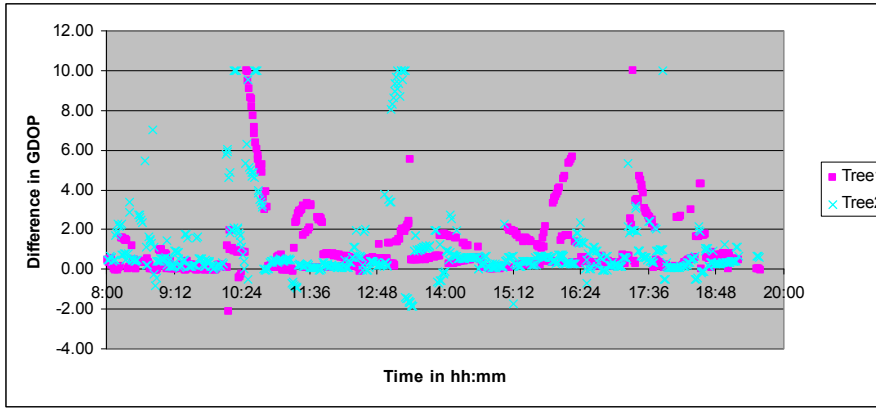

Figure 2: Difference for GDOP observed in field and computed by URP data.

The trees were also observed by Total station which was configured to yield GPS coordinates. These data are in the form of a point cloud. A convex hull was determined for these data. . To know the SVs that are actually present behind the selected trees, the extent of tree was determined in terms of minimum and maximum azimuth and elevation angles that the vertices of convex hull form at receiver location. The SVs present behind the tree were determined by using URP and the extents determined above.

The field observed SVs and SVs known to be present behind trees by URP are compared. This yields the SVs present behind a tree and actually observed by the receiver. Ratio of these two data gives the probability of a satellite being seen if it is behind a tree, earlier referred as P_{Li}. In fact this is a characteristics of the space component L_i and all SVs that are behind it will have this probability of being visible. The table 3 lists the results obtained in this experiment, which shows that P_{Li} is larger for thin canopy trees, which is obvious. In addition, to this conclusion the experiment also helps to fix the values of P_{Li} for trees depending their canopy.

Table 3: Computation of P_{Li} for a space component (here tree)

	Tree1	**Tree2**
Type of tree	Dry	Dense leaves
No. of Total Station points	552	519
No of observations of GPS	702	710
Sampling time	1 min	1 min
SVs behind tree (determined from URP)	5788	3673
SVs behind tree but visible (observed by receiver)	4607	2505
Probability P_{Li} (Ratio of above two)	0.80	0.68

5.3 LiDAR data processing

The main aim of processing LiDAR data is to classify space in components discussed above (i.e. T, L, O and G). The steps recognized for this are:

1. Space component G: This is generated by processing LiDAR data for Bare Earth Model (BEM) using known algorithms.

2. Space component O: It is assumed that all planar surfaces present in data form these components. This assumption is mostly true as the majority of obstructions which are opaque are defined by buildings etc., which are formed by planar surfaces. Hough transform based approach is proposed for this purpose.
3. Space component L: This is the set of LiDAR data points defined by $d-(g \cup o)$, where d is the set of all LiDAR data, g is the set of data classified as BEM and o is the set of data which are classified as planar surfaces. These LiDAR data represent all above ground non-planar objects, which in general are the hedges, towers, electric wires and mostly trees.
4. All L components in LiDAR data (to be identified using clustering) are given a value of P_L depending whether their canopy is thick or thin. To realise this, for all trees in study site the following ratio was determined:

$$Ratio = \left(\frac{LiDAR\ Pts.\ on\ canopy}{LiDAR\ Pts.\ on\ canopy + LiDAR\ Pts.\ below\ canopy} \right)$$

As the LiDAR data for experiment site was not available a manual judgment was made (with the help of photograph of the site of LiDAR data) to relate the experimentally determined P_L with the above ratio observed from LiDAR data as:

$P_L = 0.80$ if Ratio ≤ 0.25
$= 0.68$ if Ratio > 0.25.

LiDAR processing at present is carried out using the Terrascan software, however, the above scheme presents a potential for automating.

Tabel 4: SV combinations, their GDOP and probability for four evaluation points.

Point 1			Point 2			Point 3			Point 4		
SVs	GDOP	Prob.	SVs	GDOP	Prob.	SVs	GDOP	Prob.	SVs	GDOP	Prob.
23	NA	--	23,25,3,13,16,19,31	2.85	0.278	3,13,16,23,25	6.34	1	13,16,25,1,3,19,23,31	2.73	0.278
			23,25,3,13,16,19	4.18	0.070				13,16,25,1,3,19,23	3.45	0.070
			23,25,3,13,16,31	3.29	0.070				13,16,25,1,3,19,31	2.86	0.131
			23,25,3,13,19,31	2.94	0.070				13,16,25,1,3,23,31	2.83	0.070
			23,25,3,16,19,31	5.01	0.070				13,16,25,1,19,23,31	3.05	0.070
			23,25,13,16,19,31	3.12	0.131				13,16,25,3,19,23,31	2.85	0.070
			23,25,3,13,16	6.34	0.017				13,16,25,1,3,19	4.41	0.033
			23,25,3,16,19	6.45	0.017				13,16,25,1,19,23	3.86	0.017
			23,25,3,19,31	5.14	0.017				13,16,25,1,23,31	3.15	0.017
			23,25,3,16,31	5.07	0.017				13,16,25,1,3,23	3.54	0.017
			23,25,3,13,19	2.74	0.017				13,16,25,1,3,31	2.95	0.033
			23,25,3,13,31	3.02	0.017				13,16,25,1,19,31	3.37	0.033
			23,25,13,16,19	4.39	0.033				13,16,25,3,19,23	4.18	0.017
			23,25,13,19,31	3.21	0.033				13,16,25,3,23,31	3.29	0.017
			23,25,13,16,31	3.36	0.033				13,16,25,3,19,31	2.98	0.033
			23,25,16,19,31	8.29	0.033				13,16,25,19,23,31	3.12	0.017
			23,25,3,13	6.76	0.004				13,16,25,1,3	4.49	0.008
			23,25,3,16	15.08	0.004				13,16,25,1,19	6.18	0.008
			23,25,3,19	9.7	0.004				13,16,25,1,23	3.94	0.004
			23,25,3,31	6.05	0.004				13,16,25,1,31	3.58	0.008
			23,25,13,16	2.2	0.008				13,16,25,3,19	6.75	0.008
			23,25,13,19	5.06	0.008				13,16,25,3,23	6.34	0.004
			23,25,13,31	4.67	0.008				13,16,25,3,31	3.38	0.008
			23,25,16,19	10.66	0.008				13,16,25,19,23	4.40	0.004
			23,25,16,31	9.23	0.008				13,16,25,19,31	3.42	0.004
			23,25,19,31	8.76	0.008				13,16,25,23,31	3.77	0.008
			23,25,3	NA	0.001				13,16,25,1	7.74	0.002
			23,25,13	NA	0.002				13,16,25,3	12.65	0.002
			23,25,16	NA	0.002				13,16,25,19	9.22	0.002
			23,25,19	NA	0.002				13,16,25,23	2.20	0.001
			23,25,31	NA	0.002				13,16,25,31	6.02	0.002
			23,25	NA	0.000				13,16,25	NA	0.000

Table 5: GDOP and Probability

GDOP	Probability			
	Point 1	Point 2	Point 3	Point 4
< 3	0.00	0.37	0.00	0.62
3 to 4	0.00	0.28	0.00	0.29
4 to 5	0.00	0.11	0.00	0.06
5 to 6	0.00	0.11	0.00	0.00
6 to 7	0.00	0.04	1.00	0.02
7 to 8	0.00	0.00	0.00	0.00
> 8	1.00	0.08	0.00	0.00
Total	1.00	1.00	1.00	1.00

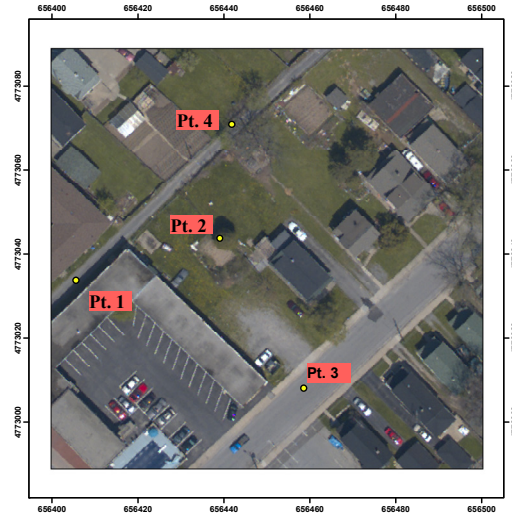

Figure 3: Study site with evaluation points

5.4 Prediction of GDOP

Using the methodology presented above the GDOP were predicted for four points as shown in figure 3. These points were chosen for their varied levels of signal masking. For various possible events (combinations of SVs that may be visible) their GDOP and the corresponding probability of success of that event are listed in table 4.

Point 1 is situated in an urban canyon like situation thus only one SV is visible at the time of GDOP determination. For Point 3 three satellites (1, 19, and 31) are behind buildings. There are no obstructions from trees. Therefore, five satellites are available for positioning giving a GDOP of 6.34 with probability of 1. In the case of points 2 and four the trees as well mask the GPS signal. The similar GDOPs are grouped in more readable format in table 5 by addition of probabilities.

6 CONCLUSION

It has been shown that the GDOP value is affected by the presence of trees in the vicinity of a receiver. URP has been used to locate all SVs that should be visible at a point in space and time. Using LiDAR data the obstructions like trees, buildings and natural topography are classified and evaluated if these would cause GPS signal masking at the receiver. Through field experiments and the LiDAR data density the translucent objects are further assigned a value that describes the probability that a satellite will be visible through them. Results presented show the correspondence between obstructions and GDOP value. The paper has introduced the concept of probability of GDOP which can help in decision making in LBS types of applications. Further work will involve more field experiment, better mathematical insight in probability description and development of a GIS based system to automate this process. Also, the effect of multipath, SNR and diffraction due to obstructions will also be included in the model.

ACKNOWLEDGEMENT

Authors thank Optech Inc. Canada for providing the LiDAR and photographic data used. Maj. Raman Kumar thanks Indian Army for permitting him PG studies at IIT Kanpur.

REFERENCES

1. Abdel-Aziz, Y.I., Karara, H.M., 1971: Direct Linear Transformation for comparator coordinates into object space coordinates in close-range photogrammetry. Proc. of ASP Symposium on Close-Range Photogrammetry, pp. 1-18
2. Germroth, M. and Carstensen, L., 2005: GIS and Satellite Visibility: Viewsheds from Space, ESRI International User Conference 2005.
3. Hasegawa, H., and Yoshimura, T., 2003: Application of dual-frequency GPS receivers for static surveying under tree canopies, J for Res., 8, 103-110.
4. MacGougan, G., Lachapelle, G., and Nayak, R., 2001: Proc. Of Overview of GNSS signal degratoin phenomena, International Symposium on Kinematic Systems in Geodesy, Geomatics and Navigation, Banff, Canada, June 5-8, 2001, 87-100.
5. Romero, I., Garcia, C., Dow, J., Zandbergen, R., 2001: Moving GPS precise orbit determination towards real-time, Proceedings GNSS 2001, Seville, Spain, May 2001 http://nng.esoc.esa.de/gps/refs/GPS_Real_Time_GNSS2001.pdf
6. Suh, Y., 2004, Development of a simulation system to evaluate the availability of satellite based navigation services using three dimesional GIS, Last accessed on 30 April 2007. http://shiba.iis.u-tokyo.ac.jp/research/Research_Outline/suh.pdf